Chapter 4

Metastable Solid Solutions of Alumina in Magnesia.

4.1 Introduction.

The previous chapter concentrated primarily on isolated defects in CeO_2. However in real materials, such as SOFC electrolytes, the situation is more complex since impurity concentrations are sufficiently high that the different defects or defect clusters can interact. Hence, we cannot assume they can be modelled as isolated species. Such interactions can crucially affect a material's properties. No doubt, both inter and intra-defect interactions would be of significance in the highly doped ceria used in fuel cells and in catalytic systems. However, the methodologies that presently exist to model such phenomena are in their infancy. Thus in the present chapter we concentrate on a simpler material which has been well characterised in the literature, both theoretically and experimentally [108], in an attempt to develop a defect interaction model which can, in future, be applied to more complex materials such as CeO_2.

The equilibrium solution limit of Al_2O_3 in MgO approaches 1% only at 1600°C[109]. Below this temperature the solubility rapidly becomes very small (≈ppm). However, at the eutectic temperature of 1995°C it is possible to dissolve up to ≈ 17wt% [109]. Materials with similar high alumina content can be formed through an alternative low temperature route [110, 111]. In this case a co-precipitate of aluminium and magnesium hydroxides is formed and calcined at 500°C . Although such materials are clearly not at equilibrium, they are kinetically stable at room temperature with respect to decomposition. In the present chapter we attempt to simulate these metastable systems by atomistic techniques.

It is important to bear in mind that in static techniques the minimised structure displacements from the original positions are very small. Hence metastable systems can be studied as the relaxation is not sufficiently large to allow the system to rearrange to its thermodynamically stable state. We compare the relaxed structures with both experimental work and other theoretical models. In particular we draw attention to the experimental work of Sato *et al.*, [110], and Rey *et al.*, [111], who determined the variation of lattice parameter as a function of defect content. Atomic scale data is provided by the work of Rohrer & Rohrer [112] who used a Monte-Carlo technique based on crystal chemical rules [113], a decidedly different technique to that used here. Nevertheless, the description by Rohrer and Rohrer of the preferential sites that the Al^{3+} ions occupy and the contraction of the lattice due to the solution of alumina, are all in agreement with the present study.

4.2 Methodology

4.2.1 Potential Parameters

The potential parameters used in the present study were chosen to reproduce the perfect lattice properties of MgO, Al_2O_3 and $MgAl_2O_4$ (see Table 4.1) and have rigorously been tested in previous work [48].

	A(eV)	ρ(Å^{-1})	C(eVÅ^6)	k(eVÅ^{-2})	Y(e)
Mg-O	1284.38	0.29969	0.0	-	-
Al-O	1725.2	0.28971	0.0	-	-
O-O	9547.96	0.2192	32.0	54.8	-2.8

Table 4.1: Interatomic potential parameters

4.2.2 Periodic Large Unit Cells Calculations

In addition to studying the perfect lattice and isolated defects, atomistic techniques can be applied to predict the energetics associated with a periodic array of defect clusters. First we create a super cell which contains 32 unit cells of the MgO lattice. Using this cell as a base, we replace a number of Mg^{2+} lattice ions with defect clusters. This allows us to simulate different concentrations of Al_2O_3 in MgO. Since the cell is repeated periodically, it is only possible to study charge neutral defect clusters. This Periodic Large Unit Cell (LUC) approach means that we are implicitly accounting for interactions between defect clusters (inter-cluster effects). From this model, since all the ion positions and unit cell vectors are relaxed to zero force, the volume of the unit cell is a well defined function of defect concentration. These calculations employed the GULP code [53].

4.2.3 Isolated Defect Model

We are additionally interested in studying the limiting case in which defect clusters are effectively isolated from each other; i.e. the inter-cluster interaction is zero and will only have an intra-cluster interaction. Isolated ion (or defect) Mott-Littleton calculations can also be used to predict lattice volumes. Clearly, such predictions totally neglect any effects of long-range defect-defect interactions. The defect relaxation volume, ν, can be calculated from [114, 72],

$$\nu = -K_T V(\delta f_v/\delta V)_T \tag{4.1}$$

where K_T is the isothermal compressibility and V the unit cell volume. $(\delta f_v/\delta V)_T$ is the change, at constant temperature, in the Helmholtz defect formation energy as a function of the change in the unit cell volume. Given the defect relaxation volume, the unit cell volume in Å can be determined from

$$\begin{array}{ccccccc} \text{Unit} & & & \text{Volume} & & \text{Concentration} & \\ \text{Cell} & = & \sum & \text{of} & \times & \text{of} & + [4.212]^3 \\ \text{Volume} & & & \text{defects} & & \text{defects} & \\ & & & & & & \\ & = & & 2\sum\nu & \times & \frac{[Al]}{[Al]+[Mg]+[Al/2]} & + [4.212]^3 \end{array}$$

where, since [Al/2] is the number of vacant cation sites assuming the reaction discussed below, [Al]+[Mg]+[Al/2] is the total number of cation sites. In this context, $\sum\nu$ is the sum of defect relaxation volumes associated with the complete solution reaction.

4.3 Solution Mechanism Of Al_2O_3 in MgO

The initial step in such investigation was to determine the solution mechanism and whether the impurities cluster. The possible solution mechanisms of Al_2O_3 into MgO, and the associated enthalpies are

$$Al_2O_3 + 3Mg_{Mg}^{X} + 3O_O^{X} \rightarrow 3MgO \ + \ 3O_O^{X} + V_{Mg}^{||} \ + \ 2Al_{Mg}^{\bullet} \qquad \Delta H = 3.42eV \tag{4.2}$$

$$Al_2O_3 \ + \ 2Mg_{Mg}^{X} + 2O_O^{X} \rightarrow 2MgO \ + \ O_i^{||} \ + \ 2Al_{Mg}^{\bullet} + \ 2O_O^{X} \qquad \Delta H = 8.69eV \tag{4.3}$$

if we assume all defects are isolated ie. no inter-defect interactions. The preferred mechanism of charge compensation, given that MgO has a dense rocksalt structure, is the formation of magnesium vacancy.

4.3.1 Defect Clusters

The aluminium substitutional ion and the magnesium vacancy are oppositely charged. Hence, their mutual Coulombic attraction results in the formation of defect clusters; either dimers, clusters containing two defect species, $(Al_{Mg}^{\bullet} : V_{Mg}^{||})^{|}$ or neutral trimers, clusters containing three defect species, $(2Al_{Mg}^{\bullet} : V_{Mg}^{||})^{X}$.

For the case of the dimer, the three nearest sites the aluminium impurity may occupy with respect to the magnesium vacancy are shown in Figure 4.1. Table 4.2 shows that the energetically favourable site is the second nearest neighbour site to the vacancy. Additionally, the result agrees with the Monte-Carlo calculations of Rohrer and Rohrer [112], who found that the second site has the greatest partial distribution function.

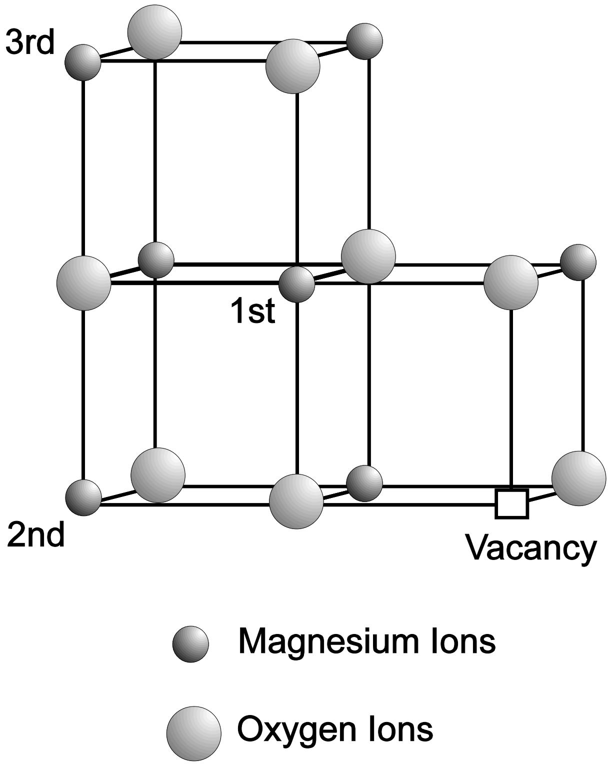

Figure 4.1: 1st, 2nd and 3rd neighbour cation sites in MgO

Position of $Al^{\bullet}_{Mg}$ with respect to $V^{||}_{Mg}$	Total energy of of defect cluster(eV)
1st neighbour	-5.72
2nd neighbour	-6.03
3rd neighbour	-5.39

Table 4.2: Defect energy of $(V^{||}_{Mg} : Al^{\bullet}_{Mg})^{|}$ dimer cluster

The case for the trimer is more complex; with respect to the $V^{||}_{Mg}$ we can consider the $Al^{\bullet}_{Mg}$ defects occupying either: $< 1st : 1st >$, $< 1st : 2nd >$, $< 1st : 3rd >$, $< 2nd : 2nd >$, $< 2nd : 3rd >$ or $< 3rd : 3rd >$ if we limit our attention to the first three neighbour sites. Within each group, the $Al^{\bullet}_{Mg}$ ions can occupy a variety of sites with respect to each other resulting in a range of Al-Al distances. Figure 4.2 shows the Coulombic energy and the unrelaxed defect energy as a function of the Al - Al distance. From this figure it is possible to conclude that the short range contribution to the unrelaxed defect energy is essentially constant and has a stabilising effect.

The most stable unrelaxed total energy is the $<1st:1st>$ configuration, with the least stable configuration being the $<2nd:3rd>$ configuration. As one would expect for a given configuration around the $V^{||}_{Mg}$, the most stable geometry is that which maximises the Al - Al distance thus reducing the Coulombic repulsion between the ions.

The situation changes on relaxation (Figure 4.3). Now the most stable configuration is that in which both the aluminium dopants are at second nearest neighbour sites with respect to the magnesium vacancy but still furthest from each other. Such a linear second neighbour site configuration is stable as it maximises the relaxation energy. In this configuration the oxygen ions adjacent to the magnesium vacancy are able to relax radially outwards from it, and simultaneously towards the $Al^{\bullet}_{Mg}$

impurities. The solution enthalpies for the reaction are thus;

$$Al_2O_3 + 3Mg_{Mg}^{X} + 3O_O^{X} \rightarrow 3MgO \ + \ V_{Mg}^{||} \ + \ 2Al_{Mg}^{\bullet} \quad \Delta H = 3.42eV \tag{4.4}$$

$$Al_2O_3 + 3Mg_{Mg}^{X} + 3O_O^{X} \rightarrow 3MgO \ + \ (V_{Mg}^{||} : Al_{Mg}^{\bullet})^{|} \ + \ Al_{Mg}^{\bullet} \ \Delta H = 2.46eV \tag{4.5}$$

$$Al_2O_3 + 3Mg_{Mg}^{X} + 3O_O^{X} \rightarrow 3MgO \ + \ (V_{Mg}^{||} : 2Al_{Mg}^{\bullet})^{X} \quad \Delta H = 1.31eV \tag{4.6}$$

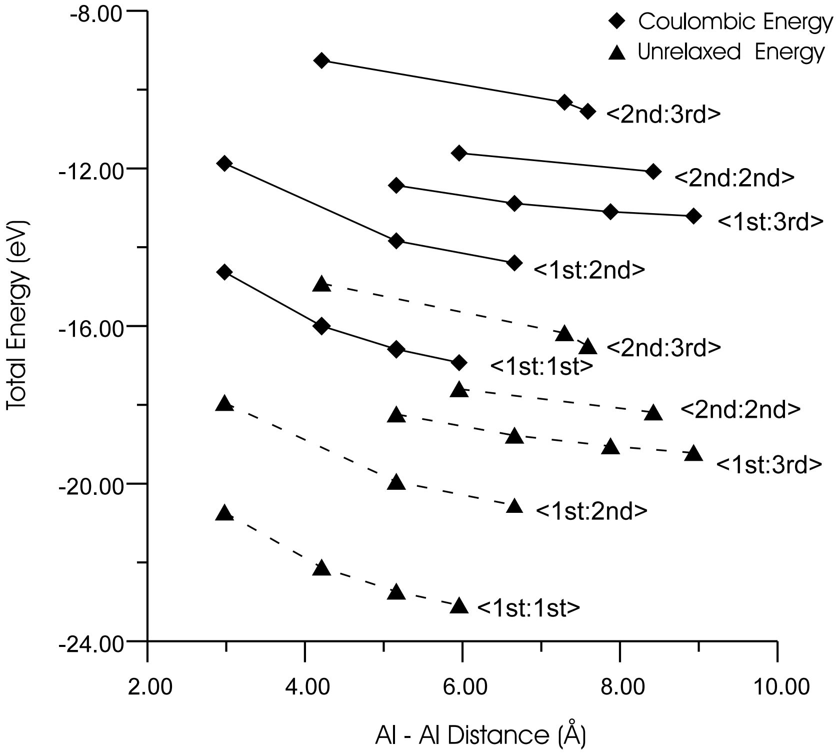

Figure 4.2: The Coulombic and unrelaxed trimer defect cluster energies

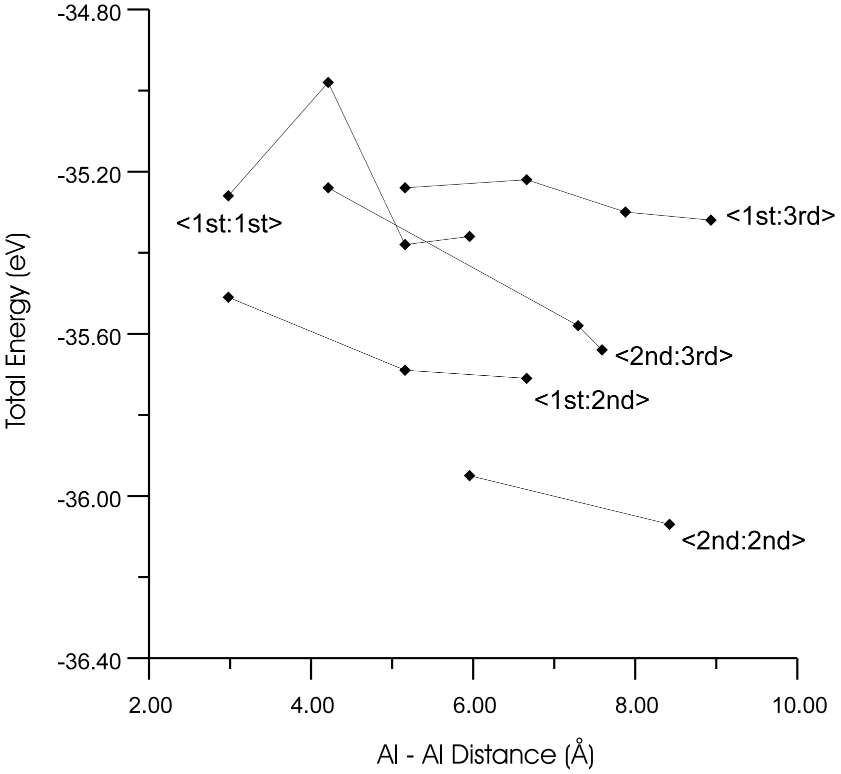

Figure 4.3: The total relaxed trimer defect cluster energies

4.4 Lattice Parameter Variation.

In the previous section we were able to determine the defect chemistry of Al_2O_3 in MgO at the infinite dilution limit. Using these results as a basis, we are in a position to examine the chemistry at higher defect concentrations. Figure 4.4 shows the predicted lattice parameter as a function of aluminium concentration for the isolated defect cluster model (intra-cluster interactions) and Figure 4.5 shows the LUC calculations (both inter- and intra-cluster effects). Also included in Figure 4.4 are the experimental values. We will assume that local rearrangements of ions are possible so that only the energetically favourable second neighbour sites for the $Al_{Mg}^{\bullet}$ ions are considered.

4.4.1 Isolated Defect Cluster Model.

Table 4.3 shows the volume change associated with the defect species predicted by the solution mechanisms in Equations 4.4, 4.5, and 4.6. If we assume that the defects exist as purely isolated entities at infinite separation (equation 4.4) then the lattice parameter is not greatly altered by increasing Al concentration.

Mechanism	Overall volume change (Å^3)
Equation 4.4	-0.72
Equation 4.5	-2.70
Equation 4.6	-3.87

Table 4.3: Sum of defect relaxation volumes

Equation 4.6 represents the scenario where the three defect species are incorporated into a single cluster. This trimer, again at infinite dilution, has the most pronounced effect on the unit cell volume due to its large negative defect volume.

The intermediate case, Equation 4.5, considers the effect of allowing partial defect clustering: two of the defects coalesce to form a dimer, whilst one of the Al ions remains as a separate species. The resultant effect on the lattice lies appropriately between the two extremes considered above.

When we compare these results with the highest concentration experimental data (see Figure 4.4) it suggests that the variation corresponds to a mixture of dimers and neutral trimers. At slightly lower concentrations the data of Sato *et al.* [110] seems to be more consistent with the existence of dimers and isolated defects. However, we must bear in mind that the experimental materials showed some evidence of spinel formation. Therefore, the concentrations should be regarded as upper limits. If this is so, this isolated defect model could be consistent with the majority of defects being neutral trimers. What is clear however is that in these non-equilibrium materials, defect clustering is necessary in order to understand the variation of the lattice parameter within the present model.

4.4.2 Periodic Large Unit Cell Calculation.

The isolated defect calculations of the last section assume implicitly that inter-cluster interactions are zero. Although this seems reasonable at very low concentrations, at the higher concentrations it cannot be true. Conversely, although LUC calculations do model intra-cluster interactions, the results can depend critically on the specific configuration being modelled despite the cell containing 256 ions. Thus it has been necessary to consider a variety of trimer defect cluster orientations, the results of which have been included in Figure 4.5. At concentrations of Al less than $\approx 8\%$ the spread of results is small and the average is in good agreement with the isolated trimer

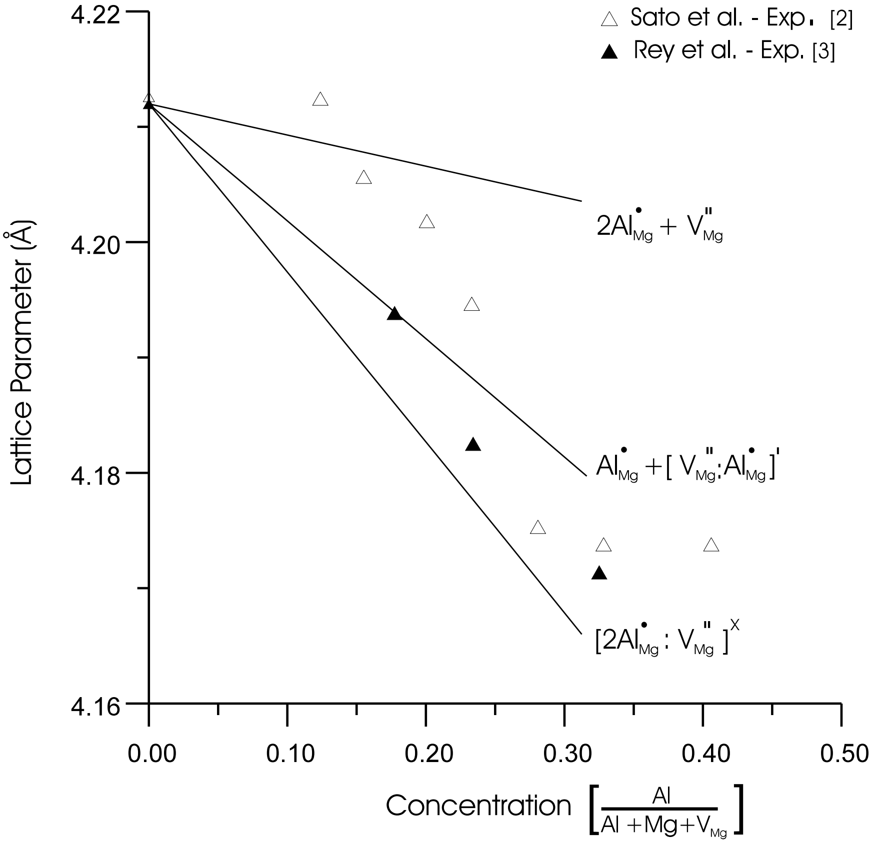

Figure 4.4: Comparison of experimental and isolated defect model lattice parameters

model. This implies that at these impurity contents the intra-cluster interactions are dominant and inter-cluster interactions are small. This is reasonable since the LUC calculations model neutral defect clusters, and the interactions between these clusters are short-range and multipole-multipole in nature.

As we proceed to concentrations of defects above 8% the spread of results increases dramatically due to the effects of inter-cluster interactions although these are sufficiently limited to suggest that intra-cluster effects are still dominant. Finally, at the highest concentrations, the inter-cluster interactions have become so strong that they are indistinguishable from the intra-cluster effects. In effect individual clusters have lost their identity and aggregate forming a super-cluster. Finally in Figure 4.5 we see that the lattice contraction predicted by Rohrer and Rohrer [112] at a concentration of 0.152, is consistent with the present LUC calculations.

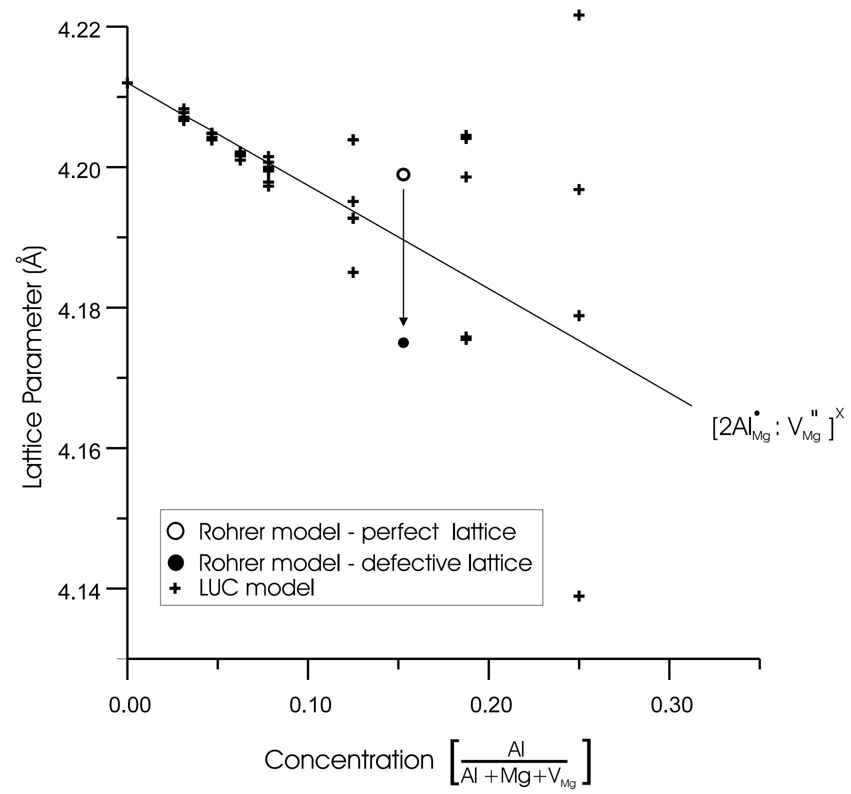

Figure 4.5: Comparison of LUC model (+) and isolated defect model lattice parameters

4.5 Summary

Static simulations have been used to predict the volume changes associated with the solution Al_2O_3 in MgO. These data are consistent with both experiment and a previous theoretical study. We assume that locally ions can move sufficiently, such that only the energetically favoured second neighbour site for the $Al^{\bullet}_{Mg}$ ion (with respect to the $V^{||}_{Mg}$) is occupied.

A model which assumes that defect clusters are isolated from each other produces an average lattice parameter which agrees with experiment at high concentrations where the inter defect cluster interactions are very significant. However at such high concentrations, different specific defect configurations within the LUC model can give rise to a wide spread of unit cell volumes. Presumably if we did not insist on trimer clusters, this variation would be even greater. To avoid this problem we would need to use a unit cell which contains thousands of ions. Unfortunately it would be computationally prohibitive to carry out a systematic study of all the possible configurations of defects in such a cell. Alternatively cells could be generated using a Monte-Carlo approach similar to that of Rohrer and Rohrer[112].

Choosing a defect configuration at high concentrations on purely energetic grounds is also flawed since the material is certainly not in equilibrium. Additionally, we have ignored configurational entropy terms which are probably significant in this type of problem. Given all the above, the isolated defect cluster model has a number of advantages and may provide a computationally efficient way of estimating the structures and lattice parameters of highly defective ceramic materials.